



Waste products from the phosphate industry as efficient removal of Acid Red 88 dye from aqueous solution: their regeneration uses and batch design adsorber

Khaled Boughzala^{a,*}, Fethi Kooli^{b,*}, Nizar Meksi^c, Ali Bechrifa^d, Khaled Bouzouita^e

^aUnité de recherche - Analyses et Procédés Appliqués à l'environnement, Institut Supérieur des Sciences Appliquées et Technologie de Mahdia, 5121 Mahdia, Tunisia, Tel. 00216 97 31 77 94; email: khaledboughzala@gmail.com (K. Boughzala)

^bDepartment of Chemistry, Faculty of Science, Islamic University of Madinah, Al-Madinah Al-Munawwarah 42351, Saudi Arabia, Tel. 00966569442963; email: fethi_kooli@yahoo.com (F. Kooli)

^cUnité de recherche de Chimie Appliquée et Environnement de Monastir, Faculté des Sciences de Monastir, 5019 Monastir, Tunisia, email: nizar_meksi@yahoo.fr (N. Meksi)

^dLaboratoire des matériaux cristallochimie et thermodynamique Appliquée, Département de Chimie, Faculté des Sciences de Tunis, Campus Universitaire, 1060 Tunis, Tunisia, email: ali.bechrifa@fst.rnu.tn (A. Bechrifa)

^eInstitut Préparatoire aux Etudes d'Ingénieur de Monastir, 5000 Monastir, Tunisia, email: khaled.bouzouita@ipeim.rnu.tn (K. Bouzouita)

Received 15 February 2020; Accepted 23 May 2020

ABSTRACT

Two waste products of the phosphate industry, phosphogypsum and phosphate waste rocks (PWR), were valorized for their use in wastewater treatment from the textile industry. Natural phosphate (PN) was also studied for comparison. First, these materials were characterized by chemical analysis, powder X-ray diffraction, Fourier-transform infrared spectroscopy, thermogravimetric analysis-differential thermal analysis, scanning electron microscopy, and N₂ adsorption isotherms. Next, they were tested as removal agents for Acid Red 88 (AR 88) dye from aqueous solution. The conducted experiments show that among the three materials, the PWR has the highest retention capacity of the dye (123.4 mg g⁻¹), and a decrease in the amount of removed AR 88 dye occurs with an increase in pH. The kinetics data on the reaction between AR 88 and the three materials are described well by a pseudo-second-order model, and the Langmuir model is successfully applied to the experimental data. The removal process is spontaneous and exothermic, accompanied by a greater distribution order of the dye molecules on the surface of the materials. Regeneration of the spent byproducts was performed by an environmentally method, and there is about an 80% removal efficiency after four cycles, depending on the spent byproducts. A single-stage batch adsorber design for AR 88 removal has been suggested and based on the Langmuir isotherm model equation.

Keywords: Natural phosphate; Phosphogypsum removal; Acidic Red 88; Regeneration; Batch design

1. Introduction

The textile, leather tanning, plastics, paper, and photoelectrochemical cell industries make use of dyes to add color to the products, and consequently, a huge amount of water is consumed [1]. Wastewater containing dyes is usually released into nearby drains, rivers, ponds, or lagoons.

Such disposal damages the quality of water bodies, the aquatic ecosystem, and the biodiversity in the environment [2,3]. This necessitates the treatment of wastewater before it is released into water streams [4]. Furthermore, the treatment of wastewater has been proposed as an alternative way to produce good-quality water for agricultural and industrial uses [5,6].

* Corresponding authors.

The removal of dyes from contaminated water can be carried out using different processes, such as ozonation, flocculation, membrane filtration, oxidation, coagulation/flocculation, photochemical or electrochemical methods, biological or photocatalytic degradation, and adsorption [7,8]. However, each technology has limitations in applicability, effectiveness, and costs [7,8]. The adsorption process is currently employed for water purification, but it remains constrained by the high price of the adsorbent materials, as well as their availability [8,9]. Proposed solutions include using alternative cheap adsorbents from agricultural residues, such as corn cob, palm fruit parts, waste material from the chestnut peel, almond shell waste, rice husk, waste orange and lime peels, pine fruit shells, and others [10,11].

Natural materials, such as clay minerals, and the waste produced by mining industries have been proposed and used for the removal of dyes [11–16]. Tunisia is considered among the top countries that produce phosphate rocks [17]. Phosphate rocks are converted into phosphoric acid by the addition of sulfuric acid through the so-called wet process [18]. Phosphogypsum (PG) is a byproduct of this process; it is produced in huge quantities, has minimal market value and presents disposal and storage problems. Thus, it is a significant source of pollution in the environment surrounding mine sites [19,20]. In addition, certain wastes are radioactive, containing different amounts of uranium and rare earth elements [21]. Some attention has been focused on the extraction of these metals for their high costs. However, the lack of an efficient and economical process to extract and recover these elements hinders efforts to reduce wastes from phosphate fertilizer production [22]. Another potential use for phosphate mining byproducts has been proposed in the last decades [23,24]. Indeed, the literature reveals the existence of a few studies related to the adsorption of some dyes in polluted textile water or adsorption of basic dyes and reactive dyes using natural phosphates (NP) [25–27].

In this study, the use of phosphate waste (PG and the solid waste phosphate waste rock (PWR) obtained from the washing process of NP) as removal agents of the Acid Red 88 (AR 88) dye was proposed. NP was used for comparison purposes. AR 88 was selected as a model dye due to its diverse applications, such as its use in the textile and leather industries. Prior to the removal study, the materials were characterized using different techniques. Different parameters were varied to study their effect on the removal of AR 88. Furthermore, the removal of dyes from wastewater produced spent materials, and a high-efficiency and the low-cost process were applied for the regeneration and the reuse of the spent materials. In addition, single-stage batch adsorber design for AR 88 removal has been suggested and based on the Langmuir isotherm equation.

2. Materials and methods

2.1. Materials

NP was collected from the Gafsa–Metlaoui Basin (denoted as the NP sample). PG is a by-product obtained from the reaction of sulfuric acid and phosphate rock. PWR is a byproduct of a phosphate company's washing plant. Prior to use, the samples were extensively washed with distilled water and then dried in an oven at 105°C. The anionic AR 88 is an acid dye and was

purchased from ATUL Limited, India; it exhibited a maximum absorption at the wavelength of 508 nm. $\text{Co}(\text{NO}_3)_2 \times 6\text{H}_2\text{O}$ and oxone ($2\text{KHSO}_5 \cdot \text{KHSO}_4 \cdot \text{K}_2\text{SO}_4$) were used without further treatment after purchasing from Alfa Aesar (4.7% active oxygen)(Alfa Aesar, Lancashire, United Kingdom).

2.2. Adsorption experiments

The removal of the AR 88 dye was performed by a batch equilibrium method. Different concentrations (varying from 5 to 200 mg L^{-1}) were obtained by diluting the stock solution (with a concentration of 1,000 mg L^{-1}). Then, 0.1 g of the solid was added to a total volume of 200 mL (dye solution) under a shaking speed of 150 rpm, natural pH, and room temperature.

The removed quantity (q_e , mg g^{-1}) and the removal percentage (R , %) were determined by Eqs. (1) and (2), respectively.

$$q_e = (C_i - C_e) \frac{V}{m} \quad (1)$$

$$R\% = \frac{(C_i - C_e)}{C_i} \times 100 \quad (2)$$

where C_i and C_e correspond to the initial and equilibrium concentrations of the AR 88 dye (mg L^{-1}). V is the used solution volume (L) and m is the material mass (mg).

In order to evaluate the effect of different parameters on the removal of AR 88, the dosage of adsorbents, contact time, initial dye concentrations, pH, and temperature were varied independently.

2.3. Regeneration of spent byproducts

Pristine NP, PG, or PWR samples were added to 200 mL of a fresh solution of AR 88 ($C_i = 200 \text{ mg L}^{-1}$) and left overnight. The spent solid was collected by centrifugation and treated with a 10 mL solution of $\text{Co}(\text{NO}_3)_2 \times 6\text{H}_2\text{O}$ and 12 mg of oxone ($2\text{KHSO}_5 \times \text{KHSO}_4 \times \text{K}_2\text{SO}_4$). The regenerated solid was centrifuged, washed a few times with deionized water, and then reused in the next run. The mixture of Co and oxone solution was not discharged and utilized in the next recycle runs [27].

2.4. Characterization

The chemical composition of the investigated materials was analyzed using atomic absorption spectroscopy (Perkin-Elmer 3110, Waltham, Massachusetts USA). Powder X-ray diffraction (XRD) analysis of the materials was carried out using an X'Pert Pro, PANalytical diffractometer (Malvern, United Kingdom) operating with Cu K α radiation. The samples were scanned from a starting angle (2θ) of 5° to an end angle (2θ) of 80°. The identification of the mineral phases was carried out using the data given in the American Society for Testing and Materials cards. Fourier-transform infrared (FTIR) spectra were obtained using a Perkin-Elmer 1283 spectrometer (Waltham, Massachusetts USA) with the KBr pellet technique. Thermal gravimetric analysis was performed using a Setaram Instrumentation (Caluire - France)

SETSYS evolution system with a heating rate of 10°C/min up to 1,000°C under an air atmosphere. The surface morphology of the samples was examined by scanning electron microscopy (SEM, FEI Quanta 200, Hillsboro, Oregon, USA). The specific surface area values were estimated from nitrogen adsorption isotherms using the Brunauer–Emmett–Teller (BET) equation. The isotherms were obtained using a Micromeritics ASAP 2020 system (Norcross, Georgia, USA). The samples were outgassed at 120°C for 8 h prior to the measurement. The pH_{zpc} of the NP, PG, and PWR samples was measured in solutions of NaCl (0.01 mol L⁻¹). The concentration of AR 88 at equilibrium was determined during the removal runs using a UV-visible spectrophotometer (Perkin-Elmer model LAMBDA20, Waltham, Massachusetts USA) at a maximum wavelength of 508 nm.

3. Results and discussion

3.1. Characterization of used materials

The results of chemical analysis are reported in Table 1. A high CaO content (45%) is present in the natural sample (NP), and it decreases to 36% and 26% in the treated samples. The NP sample exhibits a high P₂O₅ content compared with the other byproducts. A low percentage of MgO, from 0.87% to 2.15%, is detected. The atomic ratio Ca/P is between 0.34 and 1.91 for these compounds. The Cd content is a magnitude of order higher in the NP materials.

Fig. 1 shows the powder XRD patterns of the NP, PG, and PWR samples. The NP and PG patterns exhibit similar patterns. Mineralogical identification reveals the presence of carbonate fluorapatite $\text{Ca}_{9.55}(\text{PO}_4)_{4.96}\text{F}_{1.96}(\text{CO}_3)_{1.28}$ and other materials, such as heulandite $((\text{C}_2\text{H}_5)\text{NH}_{3/7.85}(\text{Al}_{8.7} \text{Si}_{27.3})\text{O}_{72}(\text{H}_2\text{O})_{6.92})$ and quartz (SiO_2). The sample of PWR exhibits different phases, such as bassanite ($\text{CaSO}_4 \cdot \frac{1}{2}\text{H}_2\text{O}$) and anhydrite (CaSO_4) compounds.

The FTIR spectra of different materials are presented in Fig. 2. The spectra of NP and PWR exhibit vibration modes of the PO₄ groups. The bands of the PO₄ groups were identified according to the literature [29]. The bands observed at 1,042 cm⁻¹ are assigned to the antisymmetric ν_3 stretching mode of the PO₄ groups. The bands related to the antisymmetric bending ν_4 modes are observed between 520 and 570 cm⁻¹. The other band at 470 cm⁻¹ corresponds to the symmetric bending ν_2 modes.

The FTIR spectrum of PG (sample PG) is characterized by the typical absorption bands reported for other gypsums or PG [30]. The bands of the SO₄ groups are detected at 1,120 cm⁻¹, 600–660 cm⁻¹ (ν_4), and 470 cm⁻¹ (ν_2). The vibration modes of the CO₃²⁻ groups are observed in the range between

1,500 and 1,400 and at 863 cm⁻¹ [31]. These bands indicate the presence of CO₃²⁻ anions in the material structure. The bands related to quartz materials overlap with those of the PO₄ groups at 1,042 cm⁻¹, with a shoulder at 474 cm⁻¹. All of the samples exhibit broad bands in the range from 3,700 to 3,000 cm⁻¹ and at 1,640 cm⁻¹, which is associated with water molecules adsorbed on the particle's surface.

The thermal features of the NP and PWR samples are given in Fig. 3. The thermogravimetric curves of the NP and PWR products display three successive mass losses. The first thermal event occurs between room temperature and 150°C and is caused by water desorption. It is associated with an endothermic effect that is observed on the differential thermal analysis (DTA) curve at 85°C and 100°C, with a shoulder at 140°C. The second mass loss corresponds to the loss of water content and dehydroxylation from 170°C

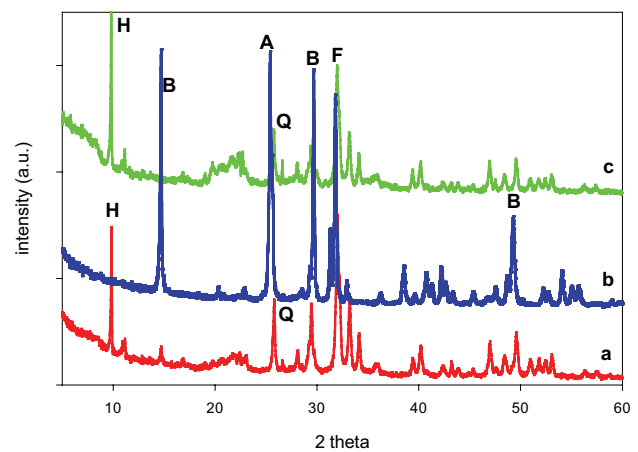


Fig. 1. Powder XRD patterns of (a) natural phosphate, (b) phosphogypsum, and (c) phosphate waste rock. (A) corresponds to anhydrite, (B) to bassanite, (H) to heulandite, (F) to carbonate fluorapatite, and (Q) to quartz phases.

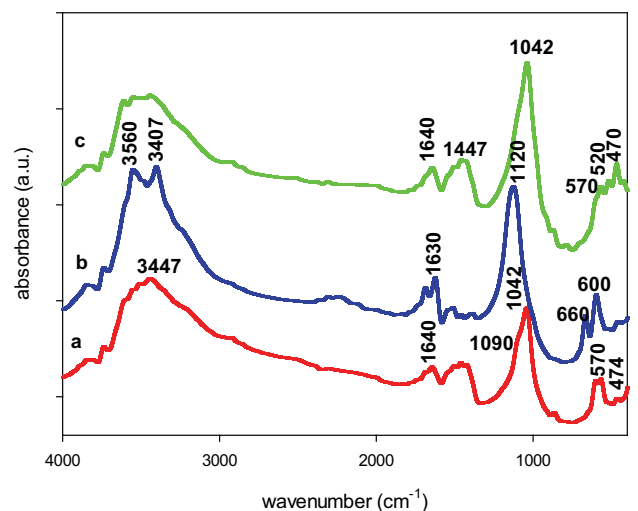


Fig. 2. FTIR spectra of (a) natural phosphate, (b) phosphogypsum, and (c) phosphate waste rock.

Table 1
Chemical analysis of the main elements in the three samples

Samples	P ₂ O ₅ (%)	CaO (%)	MgO (%)	Cd*	CaO/P ₂ O ₅
NP	25.64	44.94	0.87	45	1.75
PG	4.06	36.68	0.53	15	0.34
PWR	14.01	26.72	2.15	51	1.90

*ppm

to 450°C, with a broad endothermic effect that is evidenced on the DTA curve at around 350°C [32]. The third weight-loss event, which starts at 400°C and continues to 1,000°C, is attributed to the decomposition of carbonates and other materials [33]. Two broad exothermic peaks are detected in the range of 700°C–750°C and are associated with the phase transformation of some resulting products.

The thermogravimetric and DTA features of the PG sample are represented in Fig. 3. The thermogravimetric analysis results indicate one main mass loss between 120°C and 350°C that corresponds to the elimination of the entire water of crystallization, accompanied by an endothermic event at 207°C that is ascribed to the transition of anhydrite to different phases. A second weight loss starts at 300°C and persists until 450°C, and this is associated with the decomposition of CaSO_4 to CaO [34]. The DTA

curve exhibits broad peaks with low intensity, making their assignments difficult.

In the SEM micrographs, the NP and PWR samples exhibit nonporous particles of different sizes with spherical shapes or ovoid grains. However, for the PG sample, different shapes, such as hexagonal, tabular, and needle-like, are observed (Fig. 4).

The specific surface areas (S_{BET}) of the PG, NP, and PWR samples are 16.39, 11.35, and 26.02 $\text{m}^2 \text{g}^{-1}$, respectively, and indicate the nonporous character of these materials. The slight increase in the S_{BET} value of the PWR material could be related to the acid activation of these rocks. These values are close to those reported for NP rocks [35]. The average pore volumes are in the range of 0.023–0.053 cc g^{-1} with an average pore diameter of 9.58–7.62 nm, which confirms the nonporous character of the used materials (Table 2).

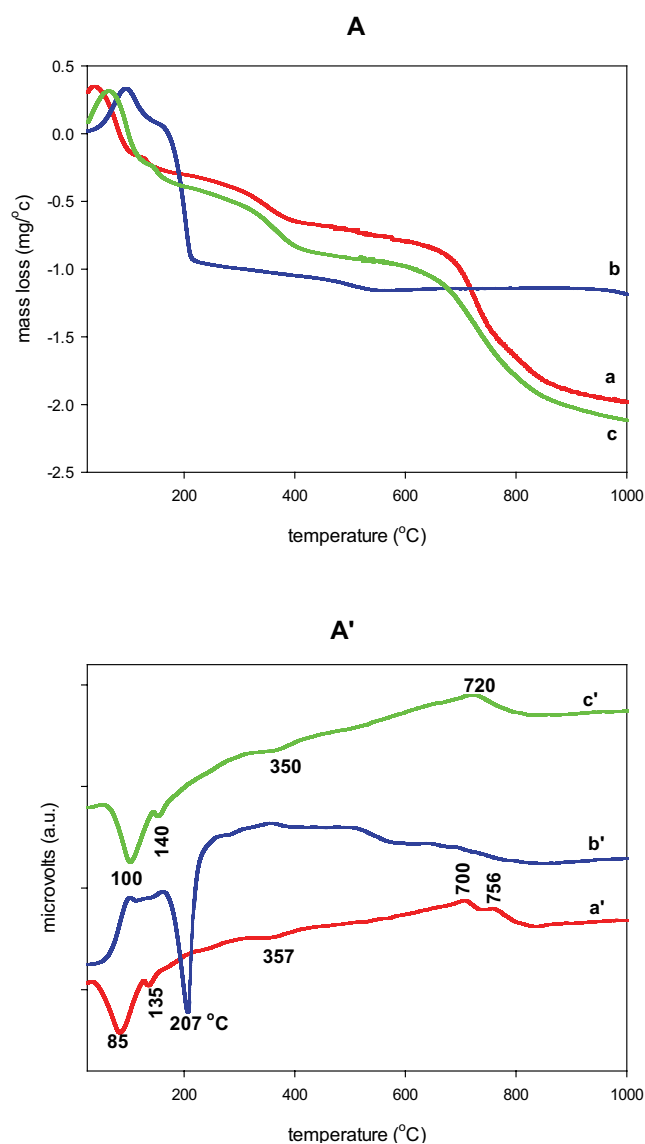


Fig. 3. (A) Thermogravimetric analysis and (A') differential thermal analysis features of (a) natural phosphate, (b) phosphogypsum, and (c) phosphate waste rock.

3.2. Removal studies

3.2.1. Effects of solid dosage

A series of runs were carried out by varying the used solid mass from 0.05 to 2 g in 200 mL of AR 88 solution (C_i of 20 mg L^{-1}). The removal efficiency (%) of NP, PG, and PWR improves as the amount of added solid increases; this is due to the greater availability of active sites on the solid's surface (Fig. 5) [36]. In particular, the PWR material exhibits a significant increase in AR 88 removal efficiency, from 44% to 99%, as the added mass of the sample increases from 0.01 to 1 g L^{-1} ; further increasing the mass of the PWR dose (from 1 to 2 g L^{-1}) does not affect the removal efficiency. However, the NP and PG materials exhibit similar removal efficiencies (99%) using a dose of 2 g L^{-1} due to their low removal capacities compared with PWR.

3.2.2. Effect of pH

The effect of pH was assessed at room temperature by adding 1 g of the NP, PG, or PWR materials to 200 mL of AR 88 solution (C_i of 100 mg L^{-1}). The mixture was stirred for 4 h. The pH was altered between 3 and 11 by adding either a solution of HCl (0.1 M) or NaOH (0.1 M).

As the pH controls the molecular structure of the adsorbates and regulates the charge distribution of the adsorbents [37], the zero charge point (p_{zpc}) was determined first. The point of zero charge (p_{zpc}) of NP, PG, and PWR is 6.89, 8.26, and 9.58, respectively. The results confirm that at pH values below $p_{\text{H}_{\text{pzc}'}}$ the surface particles are positively charged, while they become negatively charged at pH values lower than $p_{\text{H}_{\text{pzc}'}}$.

The amount of AR 88 removed by different materials generally increases when the pH decreases: the highest quantity removed was at pH 2, and it significantly decreased at pH 9 (Fig. 6). This fact is explained by the protonation of the solid surface and dye structure [38]. Indeed, at a pH equal to 3 (acidic conditions), there are significant electrostatic attractions between the $\phi\text{-SO}_3^-$ groups of the dye molecules and the positive surface charges of materials. However, at higher pH values, additional OH^- anions are available and compete with the anionic AR 88 for available

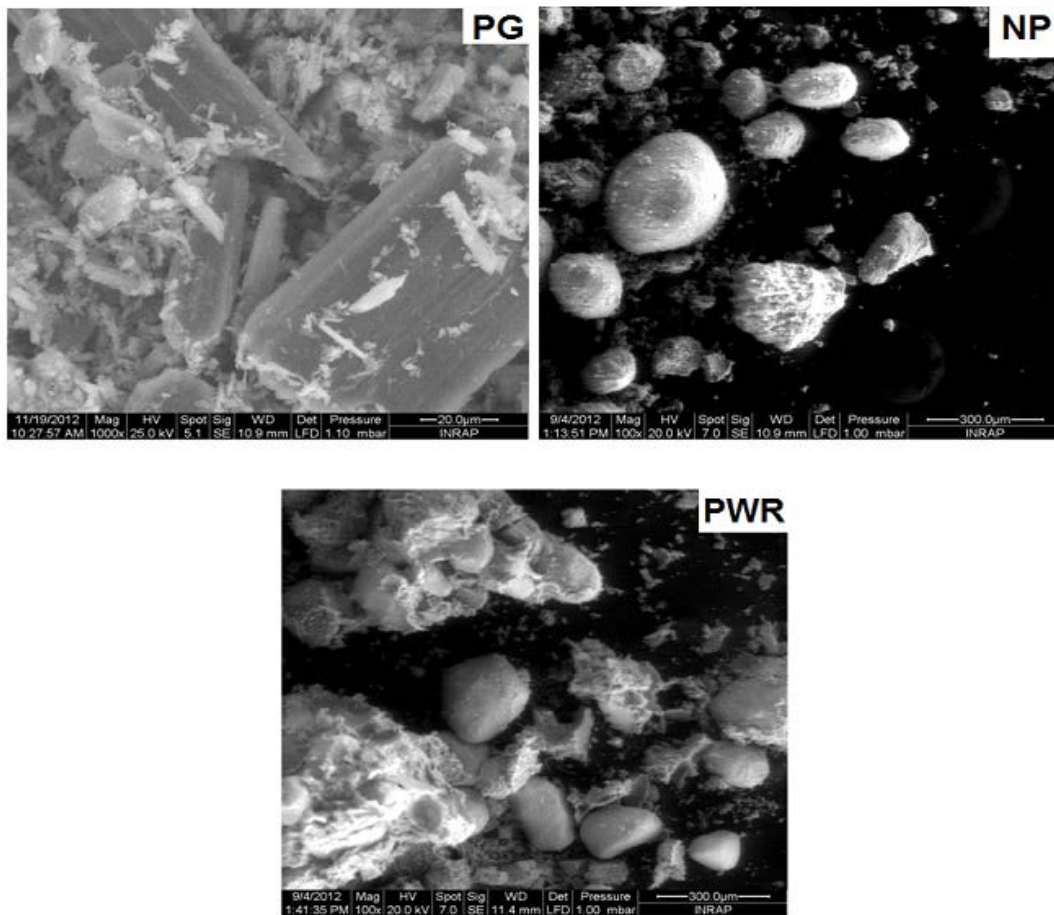


Fig. 4. SEM micrographs of (a) natural phosphate, (b) phosphogypsum, and (c) phosphate waste rock.

Table 2
Micro textural properties of the different materials

Samples	S_{BET} ($\text{m}^2 \text{g}^{-1}$)	Total pore volume (cc g^{-1})	Average pore diameter (nm)
NP	11.35	0.027	9.58
PG	16.00	0.031	7.65
PWR	26.43	0.052	7.62

sites on the NP, PG, and PWR surfaces. Thus, there is a reduction in the amount of AR 88 that can be removed.

3.2.3. Kinetics of adsorption

The effect of contact time on AR 88 removal is presented in Fig. 7. One gram of NP, PG, or PWR material was added to 200 mL of a 100 mg L^{-1} dye solution with stirring. The reaction time was set to 8 h, and 5 mL samples were taken at different time points.

The removal of AR 88 is rapid during the first time interval and becomes slower with the longer contact time, reaching a plateau after about 240 min for the NP, PG and PWR samples. This behavior can be attributed to a large number of available sites for the AR 88 dye during the initial stage.

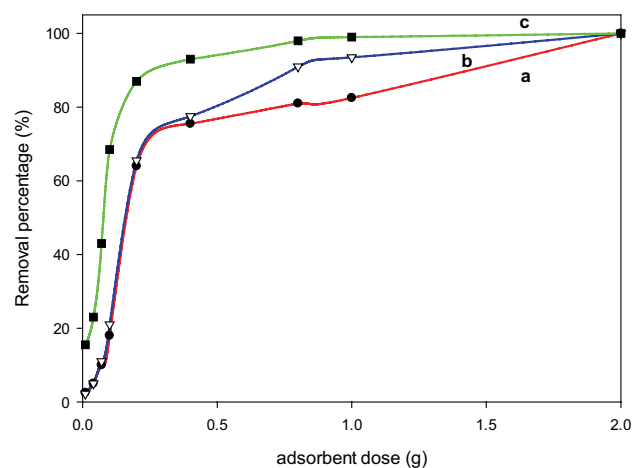


Fig. 5. Effect of dosage mass of (a) natural phosphate, (b) phosphogypsum, and (c) phosphate waste rock on the removal of AR 88 dye.

Close to equilibrium, there are fewer available sites, so they are difficult to access. In addition, the repulsive forces between the AR 88 anions on the solid and those in the solution cause the rate of adsorption to slow down [39].

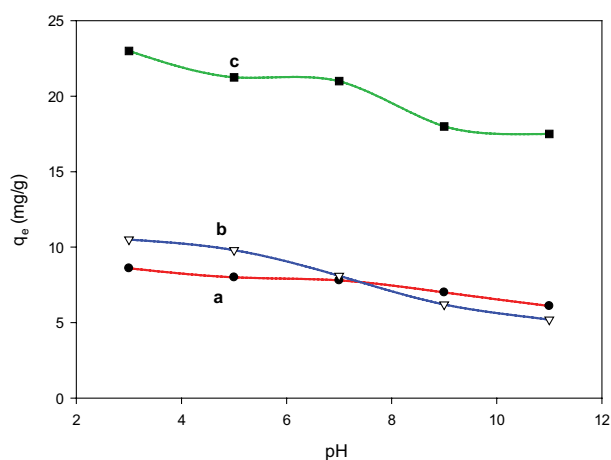


Fig. 6. Effect of initial pH on the removal of AR 88 dye by (a) natural phosphate, (b) phosphogypsum, and (c) phosphate waste rock.

3.2.3.1. Pseudo-first-order kinetic model

This model describes the rate of change that occurs for the dye uptake [40]. It is defined by Eq. (3):

$$\log(q_e - q_t) = \log q_e - \frac{k_1 t}{2.3} \quad (3)$$

where q_e and q_t are the removal capacities at equilibrium and time “ t ”, respectively. k_1 is the first-order rate constant. The linear plot of $\log(q_e - q_t)$ vs. time “ t ” shows the applicability of this model for the removal of AR 88 dye. The values of k_1 are summarized in Table 2 and vary from 0.010 to 0.014 min^{-1} . The regression correlation coefficients are close to 0.900. However, the experimental values of q_e do not match the values predicted by this model.

3.2.3.2. Pseudo-second-order kinetic model

The pseudo-second-order kinetic model is represented by Eq. (4):

$$\frac{t}{q_t} = \frac{1}{k_2 q_e^2} + \frac{t}{q_e} \quad (4)$$

where q_e and q_t are the amount of dye removed at equilibrium and at time t (mg g^{-1}), respectively. k_2 ($\text{g mg}^{-1} \text{min}^{-1}$) is the pseudo-second-order rate constant. The different parameters of the pseudo-second-order model are summarized in Table 2. Figs. 10a–d depict the linear plot of the pseudo-second-order equation. The k_2 values range in 0.005–0.008 $\text{g mg}^{-1} \text{min}^{-1}$. The estimated regression coefficient (R^2) is close to 0.9964.

The high values of the regression coefficients (R^2) and the agreement between the experimental values of q_e and the calculated ones (Table 3) indicate that the removal process of AR 88 by the NP, PG, and PWR materials is described by the pseudo-second-order model rather than the pseudo-first-order kinetic type. Similar results have been obtained for the removal of different dyes [41,42].

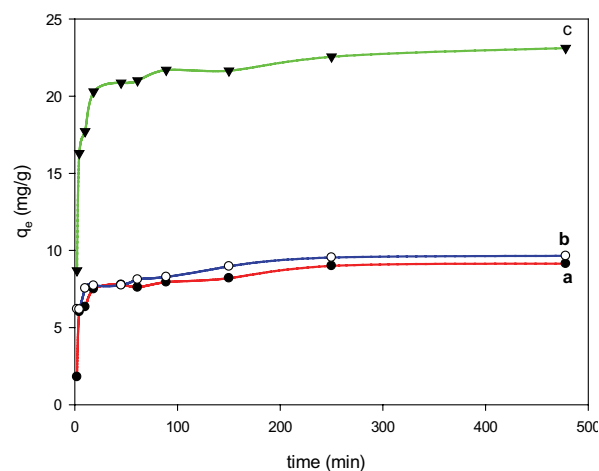


Fig. 7. Removal kinetics of AR 88 on (a) natural phosphate, (b) phosphogypsum, and (c) phosphate waste rock.

3.2.4. Effect of adsorption temperature

Temperature is a crucial parameter that affects the removal process and enables the determination of thermodynamic parameters. A series of experiments in a temperature range of 30°C–70°C were performed while maintaining the concentration of AR 88 at 200 mg L^{-1} . The removal of AR 88 decreased at equilibrium with an increase in temperature, indicating that the removal is an exothermic process [43]. Changes in thermodynamic parameters, such as (ΔG°), (ΔH°), and (ΔS°), were calculated by the following equations:

$$\Delta G^\circ = \Delta H^\circ - T\Delta S^\circ \quad (5)$$

$$\Delta G^\circ = -RT \ln K_c \quad (6)$$

$$\ln K_c = \left(\frac{\Delta S^\circ}{R} \right) - \left(\frac{\Delta H^\circ}{R} \right) \frac{1}{T} \quad (7)$$

where K_c is the distribution coefficient of AR 88 removal from aqueous solution by waste materials, “ T ” is the absolute temperature, and R is the gas constant.

Table 4 summarizes the estimated thermodynamic parameters. The negative values of ΔG° at various temperatures indicate the spontaneous nature of the removal process. The negative values of ΔH° confirm that the removal of dye using the various samples is an exothermic process. The negative ΔS° accompanying the removal of AR 88 indicates a less disordered system accompanied by a reduction in the randomness of the dye molecules at the solid–liquid interface [44,45]. The ΔG° values are $-15.33 \text{ kJ mol}^{-1}$ (for PG) and $-13.08 \text{ kJ mol}^{-1}$ (for NP), and these values represent major physical adsorption [45]. On the other hand, the removal process with PWR occurs by chemical adsorption, with a ΔG° value of $-83.13 \text{ kJ mol}^{-1}$. This process involves strong forces of attraction [46,47]. The increase in ΔG° values with temperature could be associated with a decrease in the molecular order during the removal process.

Table 3
Constant rates of pseudo-first-order and pseudo-second-order for the removal of Acid Red 88 onto various samples

Samples	Pseudo-first-order			Pseudo-second-order				
	k_1 (min ⁻¹)	q_m (mg g ⁻¹)		k_2 (min ⁻¹ g mg ⁻¹)	q_m (mg g ⁻¹)		R^2	
		Calculated	Experimental		Calculated	Experimental		
NP	0.0107	3.343	8.75	0.903	0.006	8.849	8.75	0.998
PG	0.0109	3.536	9.26	0.904	0.080	9.216	9.26	0.997
PWR	0.0144	6.855	21.875	0.900	0.005	1.796	21.875	0.996

Table 4
Thermodynamic parameters for the removal of Acid Red 88 onto various samples

Samples	ΔH° (kJ mol ⁻¹)	ΔS° (kJ mol ⁻¹)	ΔG° (kJ mol ⁻¹)	R^2
NP	-13.082	-37.805	-13.08	0.985
PG	-15.335	-48.223	-15.33	0.992
PWR	-83.133	-16.255	-83.13	0.997

3.2.5. Adsorption isotherms

Fig. 8 shows the effect of C_i on the AR 88 removal process in aqueous solutions. The obtained isotherms exhibit similar features to the enhancement in the amount of dye removed when the initial concentration was increased to a certain level, indicating the saturation of available sites on the surface of the used materials. The removed amount of AR 88 reaches 105 mg g⁻¹ when the C_i of AR 88 is 200 mg L⁻¹ for the PWR sample. For the NP and PG materials, the dye uptake decreases to 40 and 43 mg g⁻¹, respectively. This indicates that the amount of AR 88 removed by the NP, PG, and PWR materials depends on the availability of binding sites for the AR 88 dye.

The analysis of the isotherm is an important step to optimize the design of the removal process [48]. Different isotherms models were proposed in the literature [48]. The Langmuir and Freundlich are often used to describe equilibrium isotherms. The Langmuir model commonly applied to a complete homogeneous surface when the interaction between adsorbed molecules is negligible [49]. The linear equation of the Langmuir model is expressed in Eq. (8):

$$\frac{C_e}{q_e} = \frac{1}{q_{\max} \cdot K_L} + \frac{C_e}{q_{\max}} \quad (8)$$

where q_e and C_e are the removed amount of dye (mg g⁻¹) and the concentration (mg L⁻¹) in the solution at equilibrium, respectively. q_{\max} is the maximum removed amount (mg g⁻¹), and K_L (L mg⁻¹) is the Langmuir constant. The linear plot of C_e/q_e vs. C_e was used to evaluate these constants.

The Langmuir constants obtained for the NP, PG, and PWR materials are presented in Table 5. The regression correlation coefficients (R^2) are higher than 0.999. These results indicate that the removal of AR 88 by the NP, PG, and PWR materials is accurately described by the Langmuir model. The Langmuir model is also used to estimate the maximum removal capacity of the material. The estimated

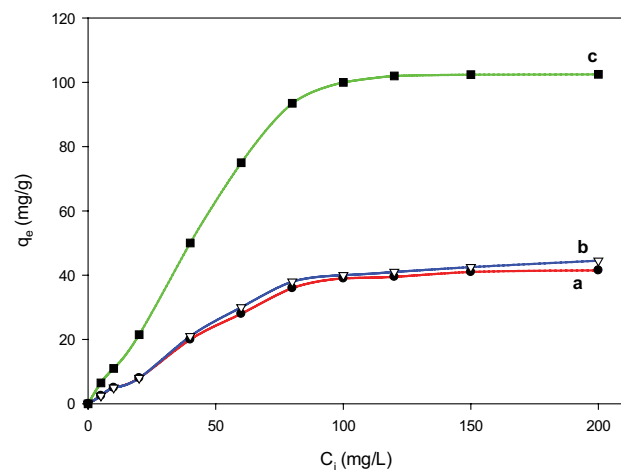


Fig. 8. Variation of the removed amount of AR 88 (q_e , mg g⁻¹) as in the function of initial concentration (C_i , mg L⁻¹) using (a) natural phosphate, (b) phosphogypsum, and (c) phosphate waste rock at room temperature.

Table 5
Langmuir and Freundlich constants, for the removal of Acid Red 88 onto various samples

Isotherm model	Parameters	NP	PG	PWR
Langmuir	$q_{m,exp}$ (mg g ⁻¹)	48.40	49.00	123.45
	K_L (L mg ⁻¹)	0.032	0.033	0.035
	R^2	0.997	0.993	0.994
Freundlich	K_f (L mg ⁻¹)	0.729	0.671	1.459
	n	0.83	0.85	0.84
	R^2	0.978	0.976	0.978

maximum removal capacities (q_m) are 48.4, 49.0, and 123.4 mg g⁻¹ for NP, PG, and PWR, respectively. Moreover, the K_L values range between 0.032 and 0.035 L mg⁻¹.

A dimensionless constant separation factor or equilibrium parameter " R_L ", a characteristic of a Langmuir isotherm, is defined in Eq. (9):

$$R_L = \frac{1}{1 + K_L C_i} \quad (9)$$

where C_i is the initial concentration (mg L^{-1}), and K_L is the Langmuir constant (L mg^{-1}). Values of R_L between zero and one ($0 < R_L < 1$) indicate that the removal is favorable; the removal is linear for $R_L = 1$, unfavorable for R_L greater than 1, and irreversible when R_L is equal to 0. In our case, R_L values were determined to be between 0 and 1, indicating the favorable adsorption of the dye to all adsorbents [51].

The removal of AR 88 by the different materials was also fitted to the Freundlich model [51] with the linear equation in Eq. (10):

$$\text{Ln}q_e = \text{Ln}K_F + \frac{1}{n}\text{Ln}C_e \quad (10)$$

where the removed amount (q_e , mg g^{-1}) is linearly related to the concentration of the AR 88 dye at equilibrium (C_e), and K_F and $1/n$ are the Freundlich constants. K_F is a combined measure of both the adsorption capacity and affinity, and $1/n$ indicates the degree or intensity of the removed AR 88 dye. The favorability of the removal is indicated by the magnitude of n , that is, values of $1/n$ less than 1 ($0 < 1/n < 1$) [51].

The values of the Freundlich parameters are presented in Table 5. The AR 88 affinity coefficient (K_F) is in the order $\text{PWR} > \text{NP} > \text{PG}$. The $1/n$ values are lower than 1, indicating that the removal of AR 88 dye is favorable under our experimental conditions.

The R^2 values obtained from the Freundlich model are around 0.971 (lower than those using the Langmuir model) indicating that the experimental data fit well to the Langmuir isotherm model. This fact reveals that, during the removal of AR 88, the dye is transferred to energetically equivalent sites, with the AR 88 molecules forming a monolayer on the outer surface of the NP, PG, and PWR materials.

3.3. Regeneration data

After the removal of AR 88, the regeneration and reutilization of the spent materials become significant to the feasibility of their use. As presented in Fig. 9, the removal efficiency is slightly reduced, from 90% to 85%, for the PWR sample for at least four runs. However, for the other two samples (NP and PG), their removal percentages decrease to 70% after three regeneration cycles. Overall, the removal efficiency is maintained at 60% for the seventh regeneration cycle. This drop in efficiency could indicate that some AR 88 molecules do not completely decompose during the regeneration process [52].

3.4. Batch design from Langmuir isotherm data

Adsorption isotherms can be used to predict the design of single-stage batch adsorption systems [53–55]. The design

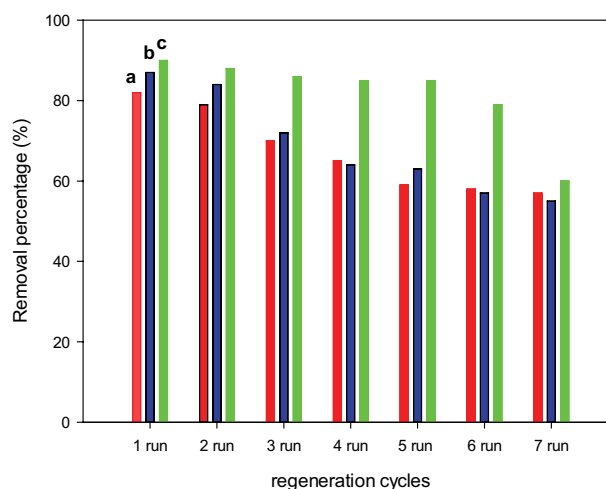


Fig. 9. Percentage removal of AR 88 after different regeneration cycles, (a) natural phosphate, (b) phosphogypsum, and (c) phosphate waste rock.

objective was to minimize the solid adsorbent for a specific volume of initial concentration [54–56].

Consider an effluent containing V (L) of the solution and let the dye concentration got reduced from C_0 to C_1 mg dye L^{-1} solution. For an amount of adsorbent m (g), the solute loading changed from q_0 to q_1 ($\text{mg dye per g adsorbent}$). When fresh adsorbent is used, $q_0 = 0$, the mass balance for the methylene blue (MB) dye in the single-stage operation under equilibrium is given by Eq. (11).

$$V(C_0 - C_e) = m(q_0 - q_e) = mq_e \quad (11)$$

In the present case, the removal of MB fitted well the Langmuir isotherm. Consequently, the Langmuir equation can be substituted in the Eq. (5), and the rearranged form is presented in Eq. (12) [56].

$$\frac{m}{V} = \frac{C_0 - C_e}{q_e} = \frac{C_0 - C_e}{\frac{q_m K_L C_e}{1 + K_L C_e}} \quad (12)$$

Figs. 10 and 11 depict the plots derived from Eq. (6) to predict the amount of PG and PWR required (g) to treat different effluent volumes of the initial concentration of 100 mg L^{-1} for 60%, 70%, 80%, and 90% MB removal at different MB solution volumes from 1 to 12 L in 1 L increment. For a single design The amount of phosphate wastes can be predicted in the range of 11 to 78.78 g for PG and 4 to 24.97 g for PWR materials. In other words, the amount required for 90% removal of MB solution of the initial concentration of 100 mg L^{-1} , was about 78.78 g of PG, and 24.97 g of PWR solids, respectively. The lower mass's values for PWR solid were related to their higher efficiency to remove MB dyes compared to PG waste. These data indicated that these materials could promote their utility as removal agents for MB.

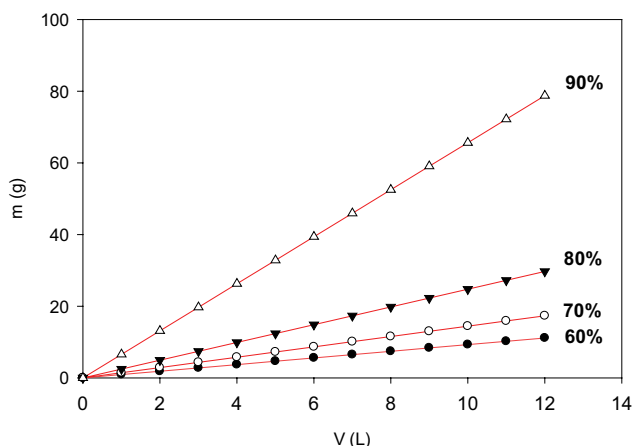


Fig. 10. Predicted mass (m) of PG waste to treat different volumes (V) of AR 88 solutions, at an initial concentration of 100 mg L^{-1} .

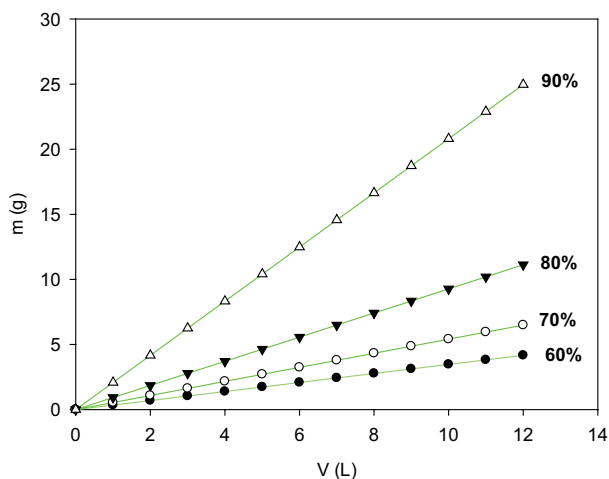


Fig. 11. Predicted mass (m) of PWR waste to treat different volumes (V) of AR 88 solutions, at an initial concentration of 100 mg L^{-1} .

4. Conclusions

The use of byproducts from the phosphate industry could create opportunities for the treatment of water contaminated by textile dyes. This study shows that NP, PG, and PWR are indeed appropriate for AR 88 removal. However, PWR (123.4 mg g^{-1}) has a removal capacity that is higher than that of the NP (48.4 mg g^{-1}) and PG (49.0 mg g^{-1}) materials. The removal is dependent on the pH of the dye solution, with higher uptake of the dye at a lower pH.

The removal rate of the AR 88 dye fits the pseudo-second-order model for all three materials. The Langmuir isotherm model more appropriately explains the experimental data compared with the Freundlich model, and it suggests the formation of a dye monolayer on the surface of the waste products. The increase in temperature resulted in a reduction in the amount of dye removed. The thermodynamic parameters revealed that the removal process is spontaneous, exothermic, and occurred via chemisorption

with the PWR. However, physisorption is the proposed mechanism of removal with NP and PG. The regeneration of spent byproducts indicates that about 80% of the removed dye was retained after four cycles for the PWR sample, and it was reduced to 60% after its reuse for seven cycles for all the materials. A batch design was proposed, based on the Langmuir model and the maximum removal capacity. The required mass of phosphate wastes to achieve a fixed percentage of MB dye removal could be readily predicted. The mass values depended on the used phosphate wastes. Due to their difference in their removal efficiency. Nevertheless, these reported data suggested that wastewater treatment is a potential application for the waste products of phosphate mining.

References

- [1] K. Hunger, R. Hamprecht, P. Miederer, C. Heid, A. Engel, K. Kunde, W. Mennicke, J. Griffiths, Chapter 3 – Dye Classes for Principal Applications, K. Hunger, Ed., Industrial Dyes: Chemistry, Properties, Applications, Wiley-VCH, Weinheim, 2004, pp. 113–338.
- [2] G.B. Michaels, D.L. Lewis, Sorption and toxicity of azo and triphenylmethane dyes to aquatic microbial populations, *Environ. Toxicol. Chem.*, 4 (1985) 45–50
- [3] S.J. Culp, F.A. Beland, Malachite green: a toxicological review, *Int. J. Toxicol.*, 15 (1996) 219–238.
- [4] A.E. Ghaly, R. Ananthashankar, M. Alhattab, V.V. Ramakrishnan, Production, characterization and treatment of textile effluents: a critical review, *J. Chem. Eng. Process. Technol.*, 5 (2014) 182, doi: 10.4172/2157-7048.1000182.
- [5] T. Asano, A.D. Levine, Wastewater reclamation, recycling and reuse: past, present, and future, *Water Sci. Technol.*, 33 (1996) 1–14.
- [6] F.R. Rijsberman, Water scarcity: fact or fiction?, *Agric. Water Manage.*, 80 (2006) 5–22.
- [7] T. Robinson, G. McMullan, R. Marchant, P. Nigam, Remediation of dyes in textile effluent: a critical review on current treatment technologies with a proposed alternative, *Bioresour. Technol.*, 77 (2001) 247–255.
- [8] H.D. Beyene, The potential of dyes removal from textile wastewater by using different treatment technology: a review, *Int. J. Environ. Monit. Anal.*, 2014 (2014) 347–353.
- [9] M.T. Yagub, T.K. Sen, S. Afroze, H.M. Ang, Dye and its removal from aqueous solution by adsorption: a review, *Adv. Colloid Interface Sci.*, 209 (2014) 172–184.
- [10] G.Z. Kyzas, J. Fu, K.A. Matis, The change from past to future for adsorbent materials in treatment of dyeing wastewaters, *Materials*, 6 (2013) 5131–5158.
- [11] M.A.M. Salleh, D.K. Mahmoud, W.A.W.A. Karim, A. Idris, Cationic and anionic dye adsorption by agricultural solid wastes: a comprehensive review, *Desalination*, 280 (2011) 1–13.
- [12] C.A.P. Almeida, A. dos Santos, S. Jaeger, N.A. Debacher, N.P. Hankins, Mineral waste from coal mining for removal of astrazon red dye from aqueous solutions, *Desalination*, 264 (2010) 181–187.
- [13] M.A. Rauf, I. Shehadeh, A. Ahmed, A. Al-Zamly, Removal of methylene blue from aqueous solution by using gypsum as a low cost adsorbent, *World Acad. Sci. Eng. Technol.*, 3 (2009) 540–545.
- [14] Y.H. Wu, J.L. Cao, P. Yilihan, Y.P. Jin, Y.J. Wen, J.X. Zhou, Adsorption of anionic and cationic dyes from single and binary systems by industrial waste lead–zinc mine tailings, *RSC Adv.*, 3 (2013) 10745–10753.
- [15] S.K. Giri, N.N. Das, G.C. Pradhan, Magnetite powder and kaolinite derived from waste iron ore tailings for environmental applications, *Powder Technol.*, 214 (2011) 513–518.
- [16] J. Cooper, R. Lombardi, D. Boardman, C. Carliell-Marquet, The future distribution and production of global phosphate rock reserves, *Resour. Conserv. Recycl.*, 57 (2011) 78–86.

- [17] P. Becker, Phosphates and Phosphoric Acid, Raw Materials Technology, and Economics of the West Process, Marcel Dekker Inc., New York, 1989.
- [18] P.M. Rutherford, M.J. Dudas, R.A. Samek, Environmental impacts of phosphogypsum, *Sci. Total Environ.*, 149 (1994) 1–38.
- [19] R. Hakkou, M. Benzaazoua, B. Bussière, Valorization of phosphate waste rocks and sludge from the Moroccan phosphate mines: challenges and perspectives, *Procedia Eng.*, 138 (2016) 110–118.
- [20] M. Azouazi, Y. Ouahidi, S. Fakhi, Y. Andres, J.Ch. Abbe, M. Benmansour, Natural radioactivity in phosphates, phosphogypsum and natural waters in Morocco, *J. Environ. Radioact.*, 54 (2001) 231–242.
- [21] H. El-Didamony, M.M. Ali, N.S. Awwad, M.M. Fawzy, M.F. Attallah, Treatment of phosphogypsum waste using suitable organic extractants, *J. Radioanal. Nucl. Chem.*, 291 (2012) 907–914.
- [22] W. Kurdowski, F. Sorrentino, Chapter 6 – Red Mud and Phosphogypsum and their Fields of Application, S. Chandra, Ed., Waste Materials Used in Concrete Manufacturing, Westwood, New Jersey, 1997, pp. 290–351.
- [23] T. Kuryatnyk, C. Angulski da Luz, J. Ambrose, J. Pera, Valorization of phosphogypsum as hydraulic binder, *J. Hazard. Mater.*, 160 (2008) 681–687.
- [24] Z. Raïs, L. El Hassani, J. Maghnouje, M. Hadji, R. Ibnelkhatay, R. Nejjar, A. Kherbeche, A. Chaqroune, Dyes' removal from textile wastewater by phosphogypsum using coagulation and precipitation method, *Phys. Chem. News*, 7 (2002) 100–109.
- [25] N. Barka, A. Assabbane, A. Nounah, L. Laanab, Y. Aït Ichou, Removal of textile dyes from aqueous solutions by natural phosphate as a new adsorbent, *Desalination*, 235 (2009) 264–275.
- [26] A. Achkoun, J. Naja, R. M'Hamdi, Elimination of cationic and anionic dyes by natural phosphate, *J. Chem. Eng.*, 6 (2012) 721–725.
- [27] F. Kooli, Y. Liu, M. Abboudi, H. Oudghiri-Hassani, S. Rakass, S.M. Ibrahim, F. Al-Wadaani, Waste bricks applied as removal agent of Basic Blue 41 from aqueous solutions: base treatment and their regeneration efficiency, *Appl. Sci.*, 9 (2019) 1237.
- [28] K. Boughzala, E. Ben Salem, A. Ben Chrifa, E. Gaudin, K. Bouzouita, Synthesis and characterization of strontium–lanthanum apatites, *Mater. Res. Bull.*, 42 (2007) 1221–1229.
- [29] A.A. Hanna, A.I.M. Akarish, S.M. Ahmed, Phosphogypsum: part I: mineralogical, thermogravimetric, chemical and infrared characterization, *J. Mater. Sci. Technol.*, 15 (1999) 431–434.
- [30] J.P. Lafon, E. Champion, D. Bernache-Assollant, Processing of AB-type carbonated hydroxyapatite $\text{Ca}_{10-x}(\text{PO}_4)_{6-x}(\text{CO}_3)_x(\text{OH})_{2-x-2y}(\text{CO}_2)_y$ ceramics with controlled composition, *J. Eur. Ceram. Soc.*, 28 (2008) 139–147.
- [31] Z. Graba, S. Hamoudi, D. Bekka, N. Bezzi, R. Boukherroub, Influence of adsorption parameters of basic red dye 46 by the rough and treated Algerian natural phosphates, *J. Ind. Eng. Chem.*, 25 (2015) 229–238.
- [32] N. Bezzi, D. Merabet, N. Benabdeslem, H. Arkoub, Caractérisation physico-chimique du minerai de phosphate de Bled el Hadba – Tebessa, *Ann. Chim. Sci. Mater.*, 26 (2001) 5–23.
- [33] S. Sebbahi, M. Lemine Ould Chameikh, F. Sahban, J. Aride, L. Benarafa, L. Belkbir, Thermal behaviour of Moroccan phosphogypsum, *Thermochim. Acta*, 302 (1997) 69–75.
- [34] H. Bouyarmane, S. Saoiabi, A. Laghzizil, A. Saoiabi, A. Rami, M. El-Karbane, Natural phosphate and its derivative porous hydroxyapatite for the removal of toxic organic chemicals, *Desal. Water Treat.*, 52 (2014) 7265–7269.
- [35] F. Kooli, L. Yan, R. Al-Faze, A. Al-Sehimi, Removal enhancement of basic blue 41 by brick waste from an aqueous solution, *Arabian J. Chem.*, 8 (2015) 333–342.
- [36] A. Chadlia, M. Mohamed Farouk, Removal of basic blue 41 from aqueous solution by carboxymethylated *Posidonia oceanica*, *J. Appl. Polym. Sci.*, 103 (2007) 1215–1225.
- [37] J.X. Lin, L. Wang, Adsorption of dyes using magnesium hydroxide-modified diatomite, *Desal. Water Treat.*, 8 (2009) 263–271.
- [38] M.J. Martin, A. Artola, M.D. Balaguer, M. Rigola, Activated carbons developed from surplus sewage sludge for the removal of dyes from dilute aqueous solutions, *Chem. Eng. J.*, 94 (2003) 231–239.
- [39] S. Lagergren, About the theory of so-called adsorption of soluble substances, *Kungliga Svenska Vetenskapsakademiens Handlingar*, 24 (1898) 1–39.
- [40] Y.S. Ho, T.H. Chiang, Y.M. Hsueh, Removal of basic dye from aqueous solution using tree fern as a biosorbent, *Process Biochem.*, 40 (2005) 119–124.
- [41] M. Doğan, M. Alkan, Adsorption kinetics of methyl violet onto perlite, *Chemosphere*, 50 (2003) 517–528.
- [42] M. Al-Ghouti, M.A.M. Khraishah, M.N.M. Ahmad, S. Allen, Thermodynamic behaviour and the effect of temperature on the removal of dyes from aqueous solution using modified diatomite: a kinetic study, *J. Colloid Interface Sci.*, 287 (2005) 6–13.
- [43] G. Rytwo, E. Ruiz-Hitzky, Enthalpies of adsorption of methylene blue and crystal violet to montmorillonite, *J. Therm. Anal. Calorim.*, 71 (2002) 751–759.
- [44] A. Ramesh, D.J. Lee, J.W.C. Wong, Thermodynamic parameters for adsorption equilibrium of heavy metals and dyes from wastewater with low-cost adsorbents, *J. Colloid Interface Sci.*, 291 (2005) 588–592.
- [45] W.J. Weber Jr, P.M. McGinley, L.E. Katz, Sorption phenomena in subsurface systems: concepts, models and effects on contaminant fate and transport, *Water Res.*, 25 (1991) 499–528.
- [46] M.A. Ferro-García, J. Rivera-Utrilla, I. Bautista-Toledo, A.C. Moreno-Castilla, Adsorption of humic substances on activated carbon from aqueous solutions and their effect on the removal of Cr(III) ions, *Langmuir*, 14 (1998) 1880–1886.
- [47] S. Ismadji, S.K. Bhatia, Adsorption of flavour esters on granular activated carbon, *Can. J. Chem. Eng.*, 78 (2000) 892–901.
- [48] K.H. Foo, B.H. Hameed, Insights into the modeling of adsorption isotherm systems, *Chem. Eng. J.*, 156 (2010) 2–10.
- [49] I. Langmuir, The adsorption of gases on plane surfaces of glass, mica and platinum, *J. Am. Chem. Soc.*, 40 (1918) 1361–1403.
- [50] K.R. Hall, L.C. Eagleton, A. Acrivos, T. Vermeulen, Pore- and solid-diffusion kinetics in fixed-bed adsorption under constant-pattern conditions, *Ind. Eng. Chem. Res.*, 5 (1966) 212–223.
- [51] O. Hamdaoui, E. Naffrechoux, Modeling of adsorption isotherms of phenol and chlorophenols onto granular activated carbon: part I. Two-parameter models and equations allowing determination of thermodynamic parameters, *J. Hazard. Mater.*, 147 (2007) 381–394.
- [52] F. Kooli, Y. Liu, M. Abouddi, S. Rakass, H. Oudgiri Hassani, S.M. Ibrahim, R. Al-Faze, Application of organo-magadiites for the removal of eosin dye from aqueous solutions: thermal treatment and regeneration, *Molecules*, 23 (2018) 2280.
- [53] G. McKay, M.S. Otterburn, J.A. Aga, Fuller's earth and fired clay as adsorbents for dyestuffs: equilibrium and rate studies, *Water Air Soil Pollut.*, 24 (1985) 307–322.
- [54] M. Özacar, İ. Ayhan Şengil, Adsorption of reactive dyes on calcined alunite from aqueous solutions, *J. Hazard. Mater.*, 98 (2003) 211–224.
- [55] V. Vadivelan, K.V. Kumar, Equilibrium, kinetics, mechanism, and process design for the sorption of methylene blue onto rice husk, *J. Colloid Interface Sci.*, 286 (2005) 90–100.